



Universiteit
Leiden
The Netherlands

Caging ruthenium complexes with non-toxic ligands for photoactivated chemotherapy

Cuello Garibo, J.A.

Citation

Cuello Garibo, J. A. (2017, December 19). *Caging ruthenium complexes with non-toxic ligands for photoactivated chemotherapy*. Retrieved from <https://hdl.handle.net/1887/58688>

Version: Not Applicable (or Unknown)

License: [Licence agreement concerning inclusion of doctoral thesis in the Institutional Repository of the University of Leiden](#)

Downloaded from: <https://hdl.handle.net/1887/58688>

Note: To cite this publication please use the final published version (if applicable).

Cover Page



Universiteit Leiden



The handle <http://hdl.handle.net/1887/58688> holds various files of this Leiden University dissertation.

Author: Cuello Garibo J.A

Title: Caging ruthenium complexes with non-toxic ligands for photoactivated chemotherapy

Issue Date: 2017-12-19

3

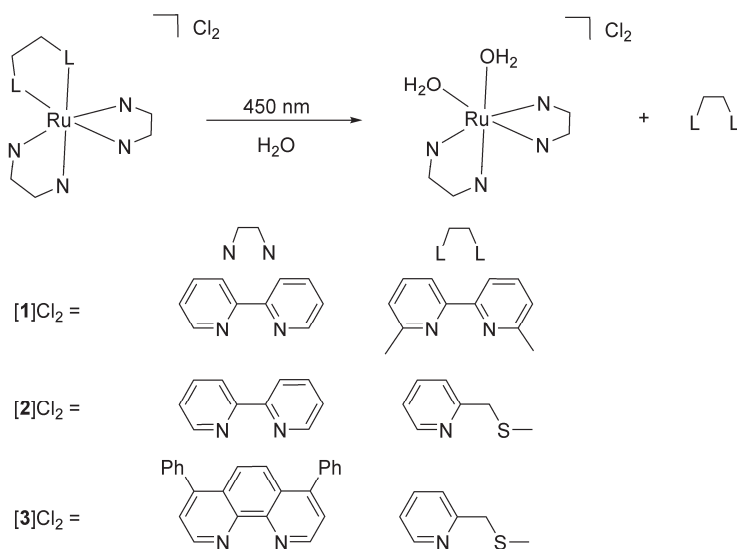
To cage or to be caged? The cytotoxic species in ruthenium-based photoactivated chemotherapy is not always the metal

In metal-based Photoactivated Chemotherapy (PACT), two photoproducts are generated by light-triggered photosubstitution of a metal-bound ligand: the dissociated ligand and an aquated metal complex. By analogy with cisplatin, the aquated metal complex is usually presented as the biologically active species, as it can typically bind to DNA. In this work, we show that this qualitative assumption is not necessarily valid by comparing the biological activity, logP, and cellular uptake of three ruthenium-based PACT complexes, $[\text{Ru}(\text{bpy})_2(\text{dmbpy})]^{2+}$, $[\text{Ru}(\text{bpy})_2(\text{mtmp})]^{2+}$, and $[\text{Ru}(\text{Ph}_2\text{phen})_2(\text{mtmp})]^{2+}$. For the first complex, the photoreleased dmbpy ligand is responsible for the observed phototoxicity, whereas the second complex is not phototoxic, and for the third complex it is the ruthenium bis-aqua photoproduct that is the sole cytotoxic species.

This chapter was published as a communication: J. A. Cuello-Garibo, M. S. Meijer, S. Bonnet *Chem. Commun.*, **2017**, 53, 6768-6771.

3.1 Introduction

Ruthenium polypyridyl complexes are well known for their versatile and tunable photophysical and photochemical properties.¹⁻⁴ In recent years, they have raised much interest for application in molecular imaging and photopharmacology,⁵⁻⁷ and in particular for Photodynamic Therapy (PDT) and Photoactivated Chemotherapy (PACT).⁸⁻⁹ In PACT, like in PDT, a non-toxic or poorly cytotoxic prodrug becomes much more cytotoxic upon light irradiation, allowing for a time- and spatially-resolved delivery of the toxicity of the anticancer drug. Whereas in PDT the photocytotoxicity relies on the photochemical generation of reactive oxygen species (ROS) such as singlet oxygen ($^1\text{O}_2$), in PACT a photochemical bond-breaking reaction occurs, which for coordination compounds is often realized *via* the photosubstitution of one of the ligands by water molecules.¹⁰⁻¹¹ To synthesize ruthenium-based compounds for PACT, $[\text{Ru}(\text{bpy})_3]^{2+}$ -like complexes (bpy = 2,2'-bipyridine) must be modified in such a way that the triplet metal-centered excited states (^3MC) comes in close proximity to the triplet metal-to-ligand charge transfer states ($^3\text{MLCT}$).¹²⁻¹³ Such modification typically entails the use of sterically hindering bidentate ligands such as 6,6'-dimethyl-2,2'-bipyridine (dmbpy) and its derivatives.¹⁴⁻¹⁵ For example, irradiation of $[\text{Ru}(\text{bpy})_2(\text{dmbpy})]^{2+}$ in water leads to the photosubstitution of dmbpy by two water molecules, generating the aquated species *cis*- $[\text{Ru}(\text{bpy})_2(\text{OH}_2)_2]^{2+}$ (Scheme 3.1), which was shown to bind to plasmid DNA.¹⁶ When performed in presence of growing cancer cells, this photoreaction clearly leads to photocytotoxicity, which many have interpreted to be a consequence of the cytotoxicity of *cis*- $[\text{Ru}(\text{bpy})_2(\text{OH}_2)_2]^{2+}$, by analogy to the cytotoxic aquated form of cisplatin, *cis*- $[\text{Pt}(\text{NH}_3)_2(\text{OH}_2)_2]^{2+}$. On the other hand, ruthenium polypyridyl complexes have also been used as photocaging groups for neurotransmitters and organic enzyme inhibitors,¹⁷⁻²¹ for which the absence of acute toxicity is a prerequisite. The parent compound $[\text{Ru}(\text{bpy})_2\text{Cl}_2]$, which thermally hydrolyzes to *cis*- $[\text{Ru}(\text{bpy})_2(\text{OH}_2)_2]^{2+}$, was shown by Reedijk and co-workers not to be cytotoxic.²²



Scheme 3.1. Chemical structures of PACT ruthenium compounds $[1]Cl_2 - [3]Cl_2$ and their reaction upon blue light irradiation in water.

As several groups have designed analogues of $[Ru(bpy)_2(dmbpy)]^{2+}$ for developing new PACT compounds, we asked ourselves which photoproducts, from the two that are formed upon light irradiation, actually are cytotoxic enough to kill cancer cells: the *cis* bis-aqua ruthenium complex, or the free ligand? To address this question, we compared the known compound $[Ru(bpy)_2(dmbpy)]Cl_2$ ($[1]Cl_2$) to the photoactive compound $[Ru(bpy)_2(mtmp)]Cl_2$ ($[2]Cl_2$) containing the bidentate chelating ligand 2-(methylthio)methylpyridine (mtmp) (Scheme 3.1).⁷ Sulfur is a soft donor atom that coordinate well to ruthenium(II) ions in the ground state, but they can be photosubstituted more efficiently than pyridines due to the relative lability of the Ru-S bond in the excited state, compared to Ru-N bonds.²³

3.2 Results and discussion

When a solution of $[2]Cl_2$ is irradiated with blue light (445 nm), a shift of the 1MLCT absorption maximum from 432 nm to 491 nm was observed, as well as two consecutive isosbestic points at 439 nm and 458 nm (Figure 3.1a). Mass spectrometry of the reaction mixture after 50 min irradiation (Figure AIV.1) showed peaks at $m/z = 140.2$, 225.0, and 448.1, which correspond to $\{mtmp + H\}^+$ (calcd $m/z = 140.2$), $[Ru(bpy)_2(OH_2)_2]^{2+}$ (calcd $m/z = 225.0$), and $[Ru(bpy)_2(OH_2)(OH)]^+$ (calcd $m/z = 448.5$), respectively. Thus, light irradiation of $[2]^{2+}$, like $[1]^{2+}$, leads to the formation of the bis-aqua complex *cis*- $[Ru(bpy)_2(OH_2)_2]^{2+}$, but the free ligand obtained as second

photoproduct is mtmp, instead of dmbpy with $[1]Cl_2$ (Scheme 3.1). The two sequential isosbestic points observed by UV-vis during irradiation of $[2]Cl_2$ suggest that photosubstitution is taking place in a two-step process. The first process is very fast (it was completed within the first 30 s of irradiation) and is assumed to be the photosubstitution of one coordination bond of mtmp by a single water molecule. The second photosubstitution was much slower, as usually reported for two monodentate ligands,²⁴ and leads to the final photoproducts mtmp and $cis-[Ru(bpy)_2(OH_2)_2]^{2+}$. The quantum yield of this second process (Φ_{PR}) is 0.0030 based on Glotaran global fitting (see Appendix I and Figure AIV.3).

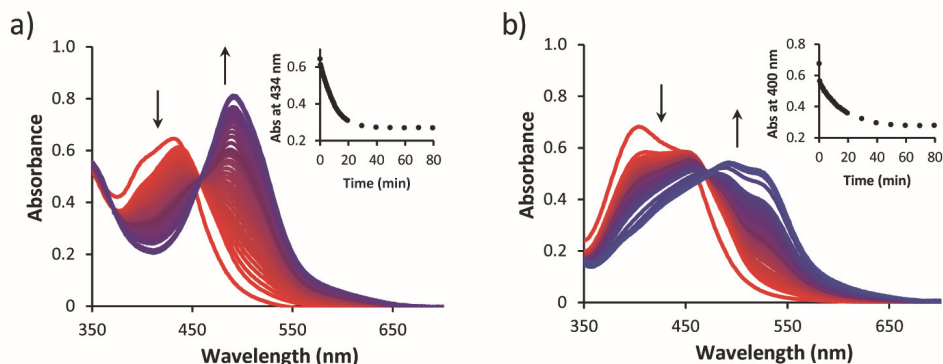


Figure 3.1. Evolution of the UV-vis absorption spectra of a solution of (a) $[2]Cl_2$ and (b) $[3]Cl_2$ in water upon irradiation with a 445 nm LED under N_2 at 25 °C. Conditions: a) 80 min, 0.109 mM, $1.49 \cdot 10^{-7} \text{ mol} \cdot \text{s}^{-1}$, b) 80 min, 0.038 mM, $1.31 \cdot 10^{-7} \text{ mol} \cdot \text{s}^{-1}$.

The cytotoxicity of the free ligands dmbpy and mtmp was first compared in A549 lung cancer cell line. Both organic ligands are rather lipophilic, as demonstrated by octanol/water partition coefficient values ($\log P$) of +3.29 and +1.63 for dmbpy and mtmp, respectively (Table 3.2). Both ligands are therefore expected to be taken up at least passively by the cells. The cell growth inhibition effective concentrations values (EC_{50}), *i.e.* the compound concentration at which the cell viability is reduced by 50% compared to the non-treated control, were measured following a protocol adapted from Hopkins *et al.* (see Appendix II).²⁵ Clearly, dmbpy was found to be cytotoxic, with an EC_{50} value of 8.7 and 6.5 μM in the dark and upon light irradiation, respectively (Figure 3.2 and Table 3.1), whereas no cytotoxicity was observed for mtmp up to 200 μM . Although cellular localization of chemicals may differ whether they are simply incubated with the cells, or generated inside the cells upon light irradiation of a prodrug such as $[1]Cl_2$, this result suggests that the photocytotoxicity reported for $[1]Cl_2$ may be at least partly due to the release of the dmbpy ligand.

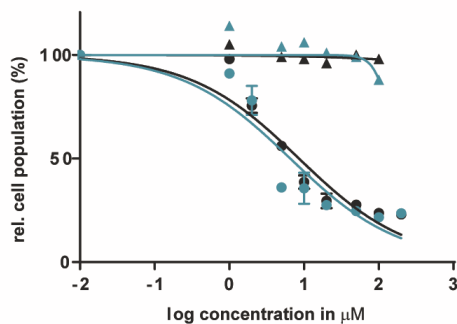


Figure 3.2. Dose-response curves for A549 cells incubated with dmbpy (circles) or mtmp (triangles) and irradiated 10 min with blue light (454 nm , $6.5\text{ J}\cdot\text{cm}^{-2}$) 6 h after treatment (blue data points), or left in the dark (black data points). Photocytotoxicity assay outline: cells seeded at $5\cdot 10^3$ cells/well at $t = 0\text{ h}$, treated with dmbpy or mtmp at $t = 24\text{ h}$, irradiated at $t = 30\text{ h}$, and SRB cell-counting assay performed at $t = 96\text{ h}$. Incubation conditions: $37\text{ }^\circ\text{C}$ and $7\%\text{ CO}_2$.

In a second step, the EC_{50} values of complexes $[1]\text{Cl}_2$ and $[2]\text{Cl}_2$ were measured in A549 cells, both in the dark and upon blue light irradiation, following the same protocol applied for the free ligand (Table 3.1). The selected light dose ($6.5\text{ J}\cdot\text{cm}^{-2}$) guarantees that no toxic effect for the cells occurs due to the irradiation itself.²⁵ At that light dose, $[1]\text{Cl}_2$ and $[2]\text{Cl}_2$ are fully activated below $40\text{ }\mu\text{M}$ (see Figure AIV.2). As shown in Figure 3.3 no significant decrease in the cell population was observed after treatment with less than $100\text{ }\mu\text{M}$ of complexes $[1]\text{Cl}_2$ or $[2]\text{Cl}_2$ in the dark (Table 3.1). Thus, these species can be considered as essentially non-cytotoxic in the dark. After blue light irradiation, an EC_{50} value of $10.9\text{ }\mu\text{M}$ was found for $[1]\text{Cl}_2$, corresponding to a photo index (PI), *i.e.* the ratio of the EC_{50} value obtained in a dark control and that obtained after light irradiation, of 19, which qualitatively fits the data reported by Glazer *et al.* on this compound.¹⁶ However, no photocytotoxicity was observed for $[2]\text{Cl}_2$, in spite of the fact that this compound also results in the formation of the *cis*- $[\text{Ru}(\text{bpy})_2(\text{OH}_2)_2]^{2+}$ species upon irradiation. In order to explain these differences, the $\log P$ value (see Experimental Section),²⁶ the cellular uptake, and the quantum yield for singlet oxygen generation were measured for both complexes (Table 3.2). $\log P$ values of -1.42 and -1.33 were found for $[1]\text{Cl}_2$ and $[2]\text{Cl}_2$, respectively, which means that both complexes have a similar hydrophilicity and are not prone to enter the cell by passive diffusion through the membrane. As expected from this high hydrophilicity, the cellular uptake before light activation was found to be very low: 1.32 and $1.27\text{ ng Ru}/10^6\text{ cells}$ for $[1]\text{Cl}_2$ and $[2]\text{Cl}_2$, respectively, compared to values usually found above $10\text{--}20\text{ ng Ru}/10^6\text{ cells}$ for compounds that are well taken up.²⁷⁻²⁸ Thus, the higher

cytotoxicity found for $[1]Cl_2$ after light activation cannot be attributed to a higher uptake of the complex prior to irradiation.

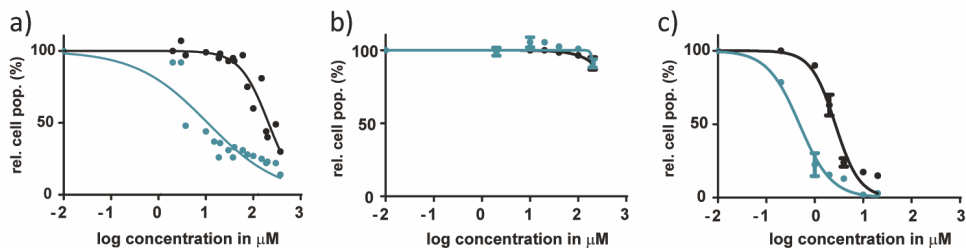


Figure 3.3. Dose-response curves for A549 cells incubated with $[1]Cl_2$ (a), $[2]Cl_2$ (b), or $[3]Cl_2$ (c) and irradiated 10 min with blue light (454 nm , $6.5\text{ J}\cdot\text{cm}^{-2}$) 6 h after treatment (blue data points), or left in the dark (black data points). Photocytotoxicity assay outline: cells seeded at $5\cdot 10^3$ cells/well at $t = 0\text{ h}$, treated with $[1]Cl_2$, $[2]Cl_2$, or $[3]Cl_2$ at $t = 24\text{ h}$, irradiated at $t = 30\text{ h}$, and SRB assay performed at $t = 96\text{ h}$. Incubation conditions: $37\text{ }^\circ\text{C}$ and $7\%\text{ CO}_2$.

Table 3.1. Cancer cell growing inhibition effective concentrations (EC_{50} values with 95% confidence interval (CI) in μM), in the dark and upon blue light irradiation ($6.5\text{ J}\cdot\text{cm}^{-2}$), for $[1]Cl_2$, $[2]Cl_2$, $[3]Cl_2$, dmbpy, and mtmp on A549 cells, and photo indices (PI) defined as $EC_{50\text{ dark}}/EC_{50\text{ light}}$.

	$[1]Cl_2$	CI (95%)	$[2]Cl_2$	CI (95%)	$[3]Cl_2$	CI (95%)	dmbpy	CI (95%)	mtmp	CI (95%)
EC_{50} dark (μM)	210	-41 +51	> 150	-	2.66	-0.46 +0.56	8.56	-2.76 +4.08	> 150	-
EC_{50} light (μM)	10.9	-4.3 +7.1	> 150	-	0.48	-0.08 +0.10	6.55	-2.54 +4.17	> 150	-
PI	19		-		6		1.3		-	

Many reported phototherapeutic ruthenium complexes are excellent PDT agents, *i.e.* they generate 1O_2 via energy transfer from the 3MLCT to molecular oxygen present in the cells.²⁹⁻³¹ Although it is commonly admitted that photosubstitutionally labile ruthenium complexes are poor singlet oxygen generators, experimental values of 1O_2 generation quantum yields (Φ_A) are rarely reported for PACT compounds. In order to rule out that $[1]Cl_2$ and $[2]Cl_2$ may act as PDT agents, Φ_A was experimentally determined for both complexes under blue light irradiation (450 nm), by direct detection of the 1274 nm infrared phosphorescence of 1O_2 in CD_3OD . Φ_A values of 0.023 and <0.005 were found for $[1]Cl_2$ and $[2]Cl_2$ (Table 3.2), respectively, using $[Ru(bpy)_3]Cl_2$ as reference ($\Phi_A = 0.73$).³² Thus, since both complexes are mediocre photosensitizers for 1O_2 , the phototoxicity of $[1]Cl_2$ cannot be due to a photodynamic effect.

To summarize, **[1]**Cl₂ and **[2]**Cl₂ have similar negative *log P* values, similarly low cellular uptake after 6 h incubation in the dark, similarly low ¹O₂ generation quantum yields, and they both form [Ru(bpy)₂(OH₂)₂]²⁺ upon light irradiation. Their main difference is that they photochemically release either dmbpy or mtmp, respectively. Meanwhile, we also demonstrated three points. First, light activation of **[1]**Cl₂ resulted in a 19-fold lower EC₅₀ value compared to the dark, whereas light irradiation of **[2]**Cl₂ does not influence the negligible cytotoxicity. Second, dmbpy is cytotoxic to A549 cells, whereas mtmp is not. Third, the EC₅₀ value of **[1]**Cl₂ after irradiation (10.9 μM) is close, in the same protocol, to the EC₅₀ value found for dmbpy (6.6 μM). All together, these results strongly suggest that the phototoxicity observed with complex **[1]**Cl₂ is caused by the dmbpy ligand that is photoreleased and taken up after extracellular activation, rather than by the *cis*-[Ru(bpy)₂(OH₂)₂]²⁺ species. In other words, [Ru(bpy)₂(OH₂)₂]²⁺ is a photocaging group for the cytotoxic dmbpy ligand, rather than the reverse.

Table 3.2. Partition coefficient (*log P* values), singlet oxygen generation quantum yields (Φ_A), and cellular uptake of **[1]**Cl₂, **[2]**Cl₂, **[3]**Cl₂, dmbpy, and mtmp.

	[1] Cl ₂	[2] Cl ₂	[3] Cl ₂	dmbpy	mtmp
<i>log P</i>	-1.42	-1.33	0.29	3.29 ^a	1.63 ^a
Φ_A	0.023	<0.005	0.020	-	-
Cellular uptake (ng Ru/10 ⁶ cells)	1.32 ± 0.06	1.27 ± 0.10	-	-	-

^a *Log P* estimation model from ChemDraw Professional (v16.0, CambridgeSoft).

These surprising results do not discredit, in our eyes, the concept of ruthenium-based PACT. The problem of compounds such as **[1]**Cl₂ or **[2]**Cl₂ is only that their ruthenium-based photoproduct, *cis*-[Ru(bpy)₂(OH₂)₂]²⁺, is not lipophilic enough to cross membranes and cause significant damage inside the cells. To demonstrate this idea, we synthesized a much more lipophilic version of compound **[2]**Cl₂, *i.e.* [Ru(Ph₂phen)₂(mtmp)]Cl₂ (**[3]**Cl₂, Ph₂phen = 4,7-Diphenyl-1,10-phenanthroline, see Scheme 3.1), by reacting [Ru(Ph₂phen)₂Cl₂] with mtmp in ethylene glycol at 115 °C. **[3]**Cl₂ has a much higher *log P* value of 0.28, as expected from the more lipophilic Ph₂phen spectator ligands. The photoreactivity of **[3]**Cl₂ in water under blue light irradiation (445 nm) is similar to that of **[2]**Cl₂: a shift of the ¹MLCT absorption maximum from 404 nm to 492 nm and two sequential isosbestic points at 447 nm and 472 nm, were observed (Figure 3.1b). Mass spectrometry of the reaction mixture after 80 min irradiation (Figure AIV.1b) also showed photosubstitution of the non-toxic mtmp ligand, with peaks at *m/z* = 140.2, 412.3, and 424.5, corresponding to {mtmp +

$H\}^+$, $[Ru(Ph_2phen)_2(CH_3CN)(OH_2)]^{2+}$ (calcd $m/z = 412.6$), and $[Ru(Ph_2phen)_2(CH_3CN)_2]^{2+}$ (calcd $m/z = 424.1$), respectively. The last two species are formed in the mass spectrometer and indicate the photochemical formation of the bis-aqua photoproduct $[Ru(Ph_2phen)_2(OH_2)_2]^{2+}$. The photosubstitution reaction has a quantum yield (Φ_{PR}) of 0.0010, slightly lower than that for $[2]Cl_2$ (Figure AIV.4), and the 1O_2 generation quantum yield was found to be similar to that for $[1]Cl_2$ (*i.e.* $\Phi_d = 0.020$, see Table 3.2). Thus, $[3]Cl_2$ is a poor PDT sensitizer but potentially a good PACT compound. Like $[2]Cl_2$, it photosubstitutes the non-toxic mtmp ligand to deliver $[Ru(Ph_2phen)_2(OH_2)_2]^{2+}$, a lipophilic analogue of $[Ru(bpy)_2(OH_2)_2]^{2+}$. In A549 cells, $[3]Cl_2$ showed a higher cytotoxicity in the dark ($EC_{50} = 2.66 \mu M$), as expected from its higher lipophilicity. The EC_{50} value decreased 6-fold down to $0.48 \mu M$ under a blue light dose of $6.5 J \cdot cm^{-2}$ (Table 3.1). Such increased cytotoxicity can, this time, only be attributed to the photochemical generation of $[Ru(Ph_2phen)_2(OH_2)_2]^{2+}$, as the second photoproduct mtmp is non-toxic. Compound $[3]Cl_2$ is thus a true metal-based PACT compound in which the toxicity of the ruthenium-based aqua species is “caged” by coordination of the mtmp ligand.

3.3 Conclusions

In conclusion, our results demonstrate that determining which photoproduct is the cytotoxic species is not straightforward, as factors such as ligand toxicity, lipophilicity of the prodrug, cellular uptake and localization, and/or 1O_2 generation, may all influence the phototoxicity of a given compound. Although we demonstrated here that the phototoxicity of $[1]Cl_2$ is not caused by the ruthenium-based photoproduct but caused by the released dmbpy ligand, compound $[3]Cl_2$ demonstrates that PACT compounds in which the ruthenium photoproduct bears the toxic load can be made, only if the lipophilicity of the compound is high enough to enter the cell.

3.4 Experimental

3.4.1 Synthesis

The ligands 6,6'-dimethyl-2,2'-bipyridine (dmbpy) and 4,7-diphenyl-1,10-phenanthroline (Ph₂phen) were purchased from Sigma-Aldrich, as well as *cis*-bis(2,2'-bipyridine)dichlororuthenium(II) hydrate (*[cis-Ru(bpy)₂Cl₂]*). Lithium chloride (LiCl) was purchased from Alfa-Aesar. All reactants and solvents were used without further purification. The synthesis of *cis*- $[Ru(Ph_2phen)_2Cl_2]$, $[1]Cl_2$, $[2]Cl_2$ and the ligand 2-(methylthio)methylpyridine was carried out according to literature procedures.^{16, 33-34}

Electrospray mass spectra (ES MS) were recorded by using a MSQ Plus Spectrometer. High resolution mass spectra were recorded by direct injection (2 μ L of 2 μ M solution in water/acetonitrile, 50/50, v/v and 0.1% formic acid) in a mass spectrometer (Thermo Finnigan LTQ Orbitrap) equipped with an electrospray (250 $^{\circ}$ C) with resolution $R = 60,000$ at m/z 400 (mass range $m/z = 150 - 2000$) and dioctylphthalate ($m/z = 391.28428$) as a lock mass. The high resolution mass spectrometer was calibrated prior to measurements with a calibration mixture (Thermo Finnigan). UV-vis experiments were performed on a Cary Varian spectrometer. All ^1H NMR spectra were recorded on a Bruker DMX-400 spectrometer. Chemical shifts are indicated in ppm relative to the residual solvent peak.

[Ru(Ph₂phen)₂(mtmp)]Cl₂ ([3]Cl₂). *cis*-[Ru(Ph₂phen)₂Cl₂] (50 mg, 0.060 mmol) was dissolved in ethylene glycol (4 mL), after which mtmp (26 mg, 0.19 mmol) and Et₃N (28 μ L, 0.20 mmol) were added. The reaction mixture was placed under N₂ atmosphere, deaerated, and heated at 115 $^{\circ}$ C for 2 h. The crude was purified by column chromatography on deactivated alumina using CH₂Cl₂ as an eluent. The orange fraction was collected and the solvent was removed by rotatory evaporation. Traces of ethylene glycol were removed by co-evaporation with toluene (30 mg, 50%). ^1H NMR (400 MHz, CD₃OD) δ 9.93 (d, $J = 5.4$ Hz, 1H), 8.80 (d, $J = 5.4$ Hz, 1H), 8.38 – 8.32 (m, 2H), 8.30 – 8.22 (m, 2H), 8.16 (d, $J = 5.5$ Hz, 1H), 8.13 (d, $J = 5.1$ Hz, 3H), 7.93 – 7.88 (m, 2H), 7.86 – 7.81 (m, 2H), 7.80 – 7.75 (m, 2H), 7.75 – 7.64 (m, 7H), 7.63 – 7.53 (m, 12H), 7.20 – 7.13 (m, 1H), 5.08 (d, $J = 16.7$ Hz, 1H), 4.61 (d, $J = 16.5$ Hz, 1H), 1.55 (s, 3H). ^{13}C NMR (101 MHz, CD₃OD) δ 154.09, 153.78, 153.50, 153.32, 152.31, 151.74, 151.59, 151.52, 150.91, 150.37, 150.11, 149.69, 149.23, 139.16, 137.07, 137.04, 136.93, 136.85, 131.21-130.24 (20C, 4 phenyl groups), 130.60, 128.17, 127.84, 127.74, 127.65, 127.57, 127.36, 127.32, 127.14, 126.43, 126.00, 16.88. High Resolution MS m/z (calcd): 452.60837 (452.60576, [3]²⁺), 940.17804 (940.18092, [3 + Cl]⁺). Anal. Calcd for C₅₅H₄₁Cl₂N₅RuS·8.5 H₂O: C, 58.51; H, 5.18; N, 6.20 Found: C, 59.56; H, 5.16; N, 5.95. UV-vis λ in nm (ϵ in M⁻¹·cm⁻¹): 405 (17300) in water.

3.4.2 Irradiation experiments monitored with MS and UV-vis

UV-vis spectroscopy was performed using a Cary Varian spectrometer equipped with a temperature control set to 298 K and a magnetic stirrer. For the irradiation a LED light source was used ($\lambda_{\text{ex}} = 445$ nm, with a Full Width at Half Maximum of 22 nm) with a photon flux of $1.49 \cdot 10^{-7}$ or $1.31 \cdot 10^{-7}$ mol·s⁻¹ (for [2]Cl₂ and [3]Cl₂, respectively). Experiments were performed in a quartz cuvette containing 3 mL of solution. A stock

solution of the desired complex was prepared using demineralized water, which was then diluted in the cuvette to the desired working concentration. When the experiment was carried out under N₂ the sample was deaerated for 15 min by gentle bubbling of N₂ and the atmosphere was kept inert during the experiment by a gentle flow of N₂ on top of the cuvette. A UV-vis spectrum was measured every 30 s for the first 10 min, every 1 min for the next 10 min, and eventually every 10 min until the end of the experiment. Data was analysed with Microsoft Excel. The quantum yields of the photoreactions (Φ_{PR}) were calculated by modelling the time evolution of the absorbance spectrum of the solution using the Glotaran software (see Appendix I, Figure AIV.3, and Figure AIV.4). Experimental conditions are detailed in Table 3.3.

Table 3.3. Conditions of the photoreactions monitored with UV-vis spectroscopy and Mass spectrometry.

Complex	Stock solution			Working solution (mM)	Photon flux 450 nm LED (mol·s ⁻¹)
	w (mg)	V (mL)	M (mM)		
[2]Cl ₂	1.0	10	0.164	0.109	1.49·10 ⁻⁷
[3]Cl ₂	1.1	10	0.113	0.038	1.31·10 ⁻⁷

3.4.3 Blue light irradiation in the cell irradiation setup

In order to assess which light dose should be used for the photocytotoxicity assay, the photochemical reactivity of [1]Cl₂ and [2]Cl₂ was tested in 96-well plates, *i.e.* in the conditions of the cell experiments, but without cells and using UV-vis spectroscopy to measure to which extent the compounds are activated at different light doses. Two solutions of each compound (40 μ M and 200 μ M) were prepared in OptiMEM complete (see Appendix II) and distributed in a 96-well plate (200 μ L per well). The plate was irradiated with blue light (454 nm) at different irradiation times (0, 2, 5, 8, 10 min) using the blue LED source described in details in Hopkins *et al.*⁶ At 40 μ M and below both complexes received enough light at 10 min irradiation (dose 6.5 J·cm⁻²) to be fully activated. At 200 μ M, complex [2]Cl₂ was only partly activated (Figure AIV.2). Higher light doses would be necessary to fully activate the highest concentrations used for [2]Cl₂, but they would also be inherently cytotoxic to A549 cells, as described in Hopkins *et al.*⁶ Thus, 10 min irradiation, for a dose of 6.5 J·cm⁻², was chosen for all photocytotoxicity experiments.

3.4.4 Partition coefficient ($\log P$)

The partition coefficient determination was adapted from Wang *et al.*²⁶ Stock solutions of [1]Cl₂, [2]Cl₂, and [3]Cl₂ were prepared in octanol-saturated water (1 mM). Aliquots of the stock solutions (0.2 mL) were transferred per triplicate to 15 mL centrifuge tubes and diluted up to 1 mL with octanol-saturated water to give 0.2 mM solutions. Then, 1 mL of water-saturated octanol was added and the mixtures were shaken in a IKA Vibrax shaker for 1 h at 2200 rpm. The mixtures were centrifuged (4300 rpm, 10 min, RT). Aliquots of the water layer (0.2 mL) were diluted with MilliQ water (2.4 mL) and 65% HNO₃ (0.4 mL) per duplicate, to give a final solution at 5% HNO₃. The ruthenium content of these samples was determined by ICP-OES using a Vista-MPX CCD Simultaneous ICP-OES. The partition coefficient values can be found in Table 3.2 and were determined by using Equation 3.1,

$$\log P_{oct} = \log \frac{[Ru]_{total} - [Ru]_{aq}}{[Ru]_{aq}}$$

Equation 3.1

where [Ru]_{total} is the concentration of ruthenium in the control sample (where no water-saturated octanol was added) and [Ru]_{aq} is the concentration of ruthenium in the aqueous layer as a mean of the six replicates.

3.4.5 Cell culture and EC₅₀ (photo)cytotoxicity assay

Following the protocol described in Appendix II, 24 h after seeding A549 cells aliquots (100 µL) of six different concentrations (2 – 200 µM for all the compounds, except for [3]Cl₂ where 0.1 – 20 µM were used) of freshly prepared stock solutions of [1]Cl₂, [2]Cl₂, [3]Cl₂, dmbpy, or mtmp in OptiMEM were added to the wells in triplicate. Plates were incubated in the dark for an additional 6 h. After this period, half of the plates were irradiated for 10 min with blue light ($\lambda = 454 \pm 11$ nm, power density = 10.5 ± 0.7 mW cm⁻², irradiation time = 10 min, light dose = 6.5 J·cm⁻²) and the other half were kept in the dark. After irradiation all the plates were incubated for an additional 66 h (making a total assay of 96 h).

3.4.6 Cellular uptake

Cell uptake studies for complexes [1]Cl₂ and [2]Cl₂ were conducted on A549 cells. $8 \cdot 10^5$ cells were seeded at $t = 0$ h in OptiMEM complete (3 mL) in 6 cm diameter

dishes. At $t = 24$ h cells were treated with solutions of [1]Cl₂ and [2]Cl₂ to give a final concentration of 20 and 80 μ M, respectively, in a total volume of 6 mL. After 6 h of drug incubation at 37 °C, the medium was aspirated and the cells were washed twice with 4 mL PBS. Then, the cells were trypsinized (1 mL), suspended with OptiMEM (3 mL), and centrifuged (1200 rpm, 4 min). After aspiration of the supernatant, the cells were resuspended in PBS (1mL) and counted. After a second centrifugation, the supernatant was discarded and the pellets were resuspended in MilliQ water (154 μ L) and 65% HNO₃ (up to 2 mL) for overnight digestion. Then, 1 mL of the solution was diluted with MilliQ water to obtain a final concentration of 5% HNO₃. For ICP-MS measurements, the system was optimized with a ruthenium-platinum solution. The calibration range was from 0 to 25 μ g/L, and obtained detection limit for all isotopes was 0.01 μ g/L. Silver and indium were used for internal standard, to correct for sample dependent matrix effects. No reference sample was available, therefore, several samples were spiked with a known concentration. The recoveries of the spiked concentrations were all within a 10% deviation. The data from two independent biological replications was used to obtain the uptake values shown in Table 3.2.

3.5 References

1. V. Balzani, G. Bergamini, F. Marchioni and P. Ceroni, *Coord. Chem. Rev.*, **2006**, 250, 1254-1266.
2. S. Campagna, F. Puntoriero, F. Nastasi, G. Bergamini and V. Balzani, *Spin Crossover In Transition Metal Compounds III*, Springer-Verlag Berlin Heidelberg, **2007**.
3. E. Baranoff, J. Collin, J. Furusho, Y. Furusho, A. Laemmel and J. Sauvage, *Inorg. Chem.*, **2002**, 41, 1215-1222.
4. E. Baranoff, J.-P. Collin, Y. Furusho, A.-C. Laemmel and J.-P. Sauvage, *Chem. Commun.*, **2000**, 1935-1936.
5. V. Fernandez-Moreira, F. L. Thorp-Greenwood and M. P. Coogan, *Chem. Commun.*, **2010**, 46, 186-202.
6. A. Martin, A. Byrne, C. S. Burke, R. J. Forster and T. E. Keyes, *J. Am. Chem. Soc.*, **2014**, 136, 15300-15309.
7. M. R. Gill, J. Garcia-Lara, S. J. Foster, C. Smythe, G. Battaglia and J. A. Thomas, *Nat Chem*, **2009**, 1, 662-667.
8. C. Mari, V. Pierroz, S. Ferrari and G. Gasser, *Chem. Sci.*, **2015**, 6, 2660-2686.
9. M. Frascioni, Z. Liu, J. Lei, Y. Wu, E. Strekalova, D. Malin, M. W. Ambrogio, X. Chen, Y. Y. Botros, V. L. Cryns, J.-P. Sauvage and J. F. Stoddart, *J. Am. Chem. Soc.*, **2013**, 135, 11603-11613.
10. R. N. Garner, J. C. Gallucci, K. R. Dunbar and C. Turro, *Inorg. Chem.*, **2011**, 50, 9213-9215.
11. B. A. Albani, B. Peña, N. A. Leed, N. A. B. G. de Paula, C. Pavani, M. S. Baptista, K. R. Dunbar and C. Turro, *J. Am. Chem. Soc.*, **2014**, 136, 17095-17101.
12. A.-C. Laemmel, J.-P. Collin and J.-P. Sauvage, *Eur. J. Inorg. Chem.*, **1999**, 383-386.
13. L. Salassa, C. Garino, G. Salassa, R. Gobetto and C. Nervi, *J. Am. Chem. Soc.*, **2008**, 130, 9590-9597.
14. T. Sainuddin, M. Pinto, H. Yin, M. Hetu, J. Colpitts and S. A. McFarland, *J. Inorg. Biochem.*, **2016**, 158, 45-54.

15. K. T. Hufziger, F. S. Thowfeik, D. J. Charboneau, I. Nieto, W. G. Dougherty, W. S. Kassel, T. J. Dudley, E. J. Merino, E. T. Papish and J. J. Paul, *J. Inorg. Biochem.*, **2014**, 130, 103-111.
16. B. S. Howerton, D. K. Heidary and E. C. Glazer, *J. Am. Chem. Soc.*, **2012**, 134, 8324-8327.
17. O. Filevich, M. Salierno and R. Etchenique, *J. Inorg. Biochem.*, **2010**, 104, 1248-1251.
18. L. Zayat, O. Filevich, L. M. Baraldo and R. Etchenique, *Philos. Trans. R. Soc., A*, **2013**, 371.
19. N. Karaoun and A. K. Renfrew, *Chem. Commun.*, **2015**, 51, 14038-14041.
20. T. Respondek, R. Sharma, M. K. Herroon, R. N. Garner, J. D. Knoll, E. Cueny, C. Turro, I. Podgorski and J. J. Kodanko, *ChemMedChem*, **2014**, 9, 1306-1315.
21. N. A. Smith, P. Zhang, S. E. Greenough, M. D. Horbury, G. J. Clarkson, D. McFeely, A. Habtemariam, L. Salassa, V. G. Stavros, C. G. Dowson and P. J. Sadler, *Chem. Sci.*, **2017**, 8, 395-404.
22. O. Novakova, J. Kasparkova, O. Vrana, P. M. Vanvliet, J. Reedijk and V. Brabec, *Biochemistry*, **1995**, 34, 12369-12378.
23. R. N. Garner, L. E. Joyce and C. Turro, *Inorg. Chem.*, **2011**, 50, 4384-4391.
24. D. V. Pinnick and B. Durham, *Inorg. Chem.*, **1984**, 23, 1440-1445.
25. S. L. Hopkins, B. Siewert, S. H. C. Askes, P. Veldhuizen, R. Zwier, M. Heger and S. Bonnet, *Photochem. Photobiol. Sci.*, **2016**, 15, 644-653.
26. F. Wang, J. Xu, A. Habtemariam, J. Bella and P. J. Sadler, *J. Am. Chem. Soc.*, **2005**, 127, 17734-17743.
27. V. H. S. van Rixel, B. Siewert, S. L. Hopkins, S. H. C. Askes, A. Busemann, M. A. Siegler and S. Bonnet, *Chem. Sci.*, **2016**, 7, 4922-4929.
28. Y. Fu, C. Sanchez-Cano, R. Soni, I. Romero-Canelon, J. M. Hearn, Z. Liu, M. Wills and P. J. Sadler, *Dalton Trans.*, **2016**, 45, 8367-8378.
29. C. Mari, V. Pierroz, R. Rubbiani, M. Patra, J. Hess, B. Spingler, L. Oehninger, J. Schur, I. Ott, L. Salassa, S. Ferrari and G. Gasser, *Chem. - Eur. J.*, **2014**, 20, 14421-14436.
30. A. Frei, R. Rubbiani, S. Tubafard, O. Blacque, P. Anstaett, A. Felgentrager, T. Maisch, L. Spiccia and G. Gasser, *J. Med. Chem.*, **2014**, 57, 7280-7292.
31. G. Shi, S. Monro, R. Hennigar, J. Colpitts, J. Fong, K. Kasimova, H. Yin, R. DeCoste, C. Spencer, L. Chamberlain, A. Mandel, L. Lilge and S. A. McFarland, *Coord. Chem. Rev.*, **2015**, 282-283, 127-138.
32. D. Garcia-Fresnadillo, Y. Georgiadou, G. Orellana, A. M. Braun and E. Oliveros, *Helv. Chim. Acta*, **1996**, 79, 1222-1238.
33. J. H. Wallenstein, J. Sundberg, C. J. McKenzie and M. Abrahamsson, *Eur. J. Inorg. Chem.*, **2016**, 897-906.
34. E. Reisner, T. C. Abikoff and S. J. Lippard, *Inorg. Chem.*, **2007**, 46, 10229-10240.

